Supplementary Materials

SARS-CoV-2 ferritin nanoparticle vaccine induces robust innate immune activity driving polyfunctional spike-specific T cell responses

Joshua M. Carmen[1]*, Shikha Shrivastava[1,2]*, Zhongyan Lu[3]*, Alexander Anderson[1,2], Elaine B. Morrison[1], Rajeshwer S. Sankhala[4,5], Wei-Hung Chen[4,5], William C. Chang[4,5], Jessica S. Bolton[6], Gary R. Matyas[1], Nelson L. Michael[7], M. Gordon Joyce [4,5], Kayvon Modjarrad[4], Jeffrey R. Currier[8], Elke Bergmann-Leitner[6], Allison M.W. Malloy[3†], and Mangala Rao[1‡]

[‡]Corresponding author. Email: mrao@hivresearch.org
[†]Co-Corresponding Author: Email: Allison.malloy@usuhs.edu

This file includes:

SUPPLEMENTARY MATERIALS

Supplementary Fig. 1. Flow cytometry analysis of innate immune cells in draining lymph nodes responding to SpFN vaccine adjuvanted with ALFQ or AH.

Supplementary Fig. 2. Characterization of the responding T cells upon priming with SpFN vaccine adjuvanted with ALFQ or AH.

Supplementary Fig. 3. Frequency of total $CD3^+$ T cells in splenocytes of mice following prime and prime boost vaccination with SpFN adjuvanted with AH or ALFQ.

Supplementary Fig. 4. Flow gating strategy to determine the frequency of cytokine secreting $CD4^+$ and $CD8^+$ T cells.

Supplementary Fig. 5. Amino acid sequence of the SARS-COV-2 spike protein.

Supplementary Fig. 6. Flow gating strategy to determine the frequency of SARS-CoV-2 spike-specific $CD8^+$ T cells in the splenocytes of mice as detected by MHC class I tetramer staining following SpFN vaccination.

Supplementary Fig. 7. Flow gating strategy to determine the frequency of SARS-CoV-2 spike-specific $CD8^+$ T cells in perfused lungs of SpFN vaccinated mice as detected by MHC class I tetramer staining followed by CD69 and CD103 staining.

Supplementary Table 1. List of antibodies used for Cytex flow cytometry-based analysis of the APC phenotypes

Supplementary Table 2. List of antibodies used for Cytex flow cytometry-based analysis of the T cell phenotypes

Supplementary Table 3. List of antibodies used for Cytex flow cytometry-based analysis of the T cell cytokine staining

Supplementary Table 4. List of antibodies used for intracellular cytokine staining by BD LSRII flow cytometry-based analysis of the cytokine response in the splenocytes

Supplementary Table 5. List of antibodies used for staining perfused lung cells and analysis by BD LSRII flow cytometry

Supplementary Table 6. List of MHC class I tetramer used for the detection of SARS-CoV-2 spike specific $CD8^+$ T cell response

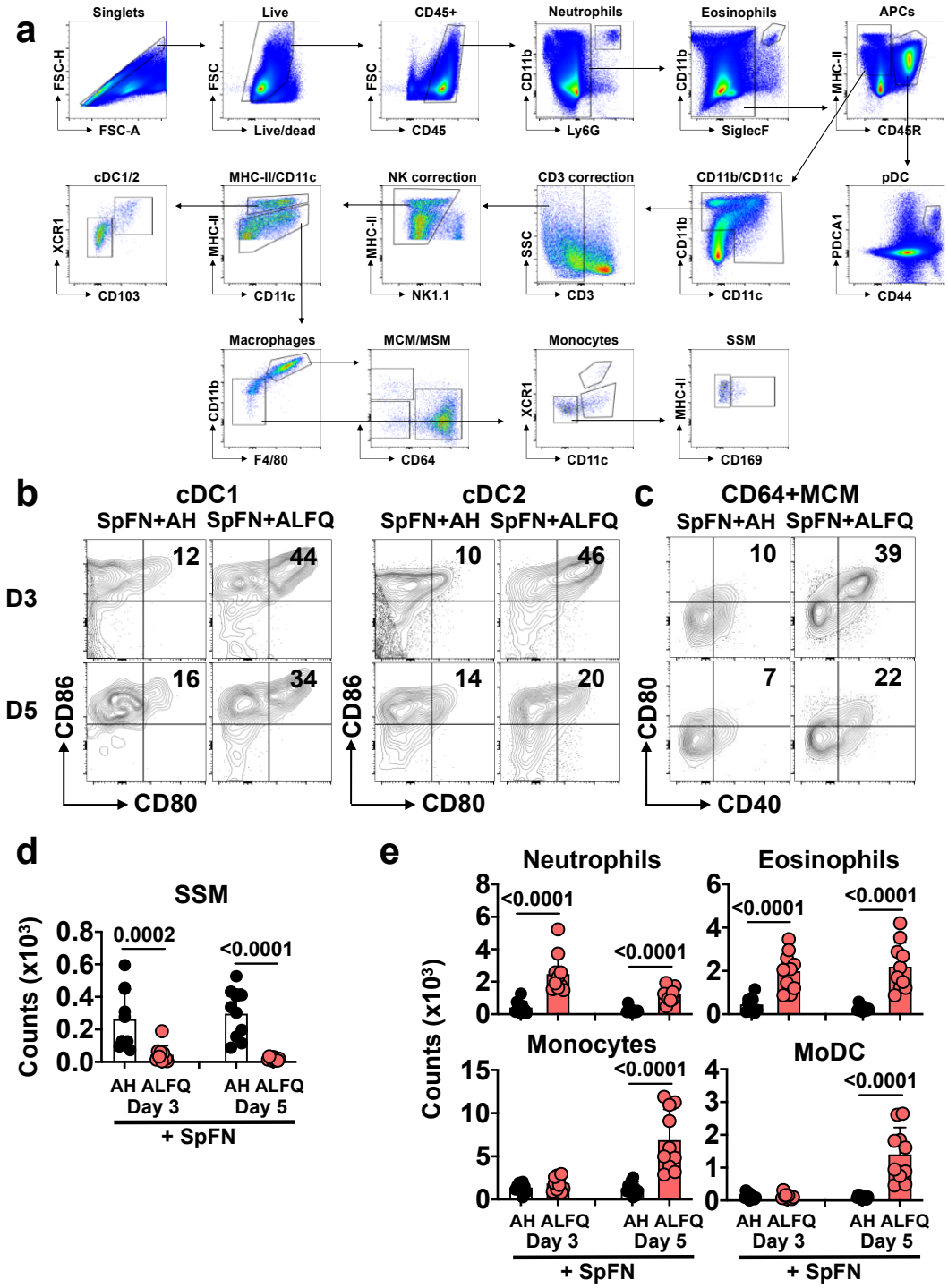

Supplementary Fig. 1. Spectral flow cytometry analysis of innate immune cells in draining lymph nodes responding to SpFN vaccine adjuvanted with ALFQ or AH.

(a) Flow cytometry gating strategy for the identification of neutrophils (Ly6G$^+$CD11b$^+$), eosinophils (Siglec F$^+$CD11b$^+$), pDCs (MHC-II$^+$CD45R$^+$PDCA1$^+$), cDC1 (MHC-II high CD11c$^+$XCR1$^+$CD103$^+$), cDC2 (MHC-II high CD11c$^+$XCR1$^-$), MSM (MHC II$^+$F4/80$^+$CD11b$^+$CD169$^+$CD64$^-$), MCM (MHC-II$^+$F4/80$^+$CD11b$^+$CD169-CD64+/-), SSM (CD11b$^+$CD169$^+$F4/80$^-$), XCR1+cDC1-like MoDCs (MHC-II+CD11b int CD11c$^+$XCR1$^+$), XCR1-CD11c$^+$MoDCs (MHC-II$^+$CD11b int CD11c$^+$XCR1$^-$), and monocytes (MHC-II$^+$CD11b int CD11c$^-$XCR1$^-$). **(b)** Flow cytometry plots demonstrating expression of costimulatory molecules CD80 and CD86 by cDC upon activation after vaccination. (**c)** Flow cytometry plots demonstrating activation of MCM by expression of CD40 and CD80. **(d)** Magnitude of SSM, and **(e)** other non-classical APCs, including neutrophils, eosinophils, XCR1$^+$MoDCs, and monocytes at days 3 and 5 post priming vaccination. Bars indicate mean $\pm$ s.d.

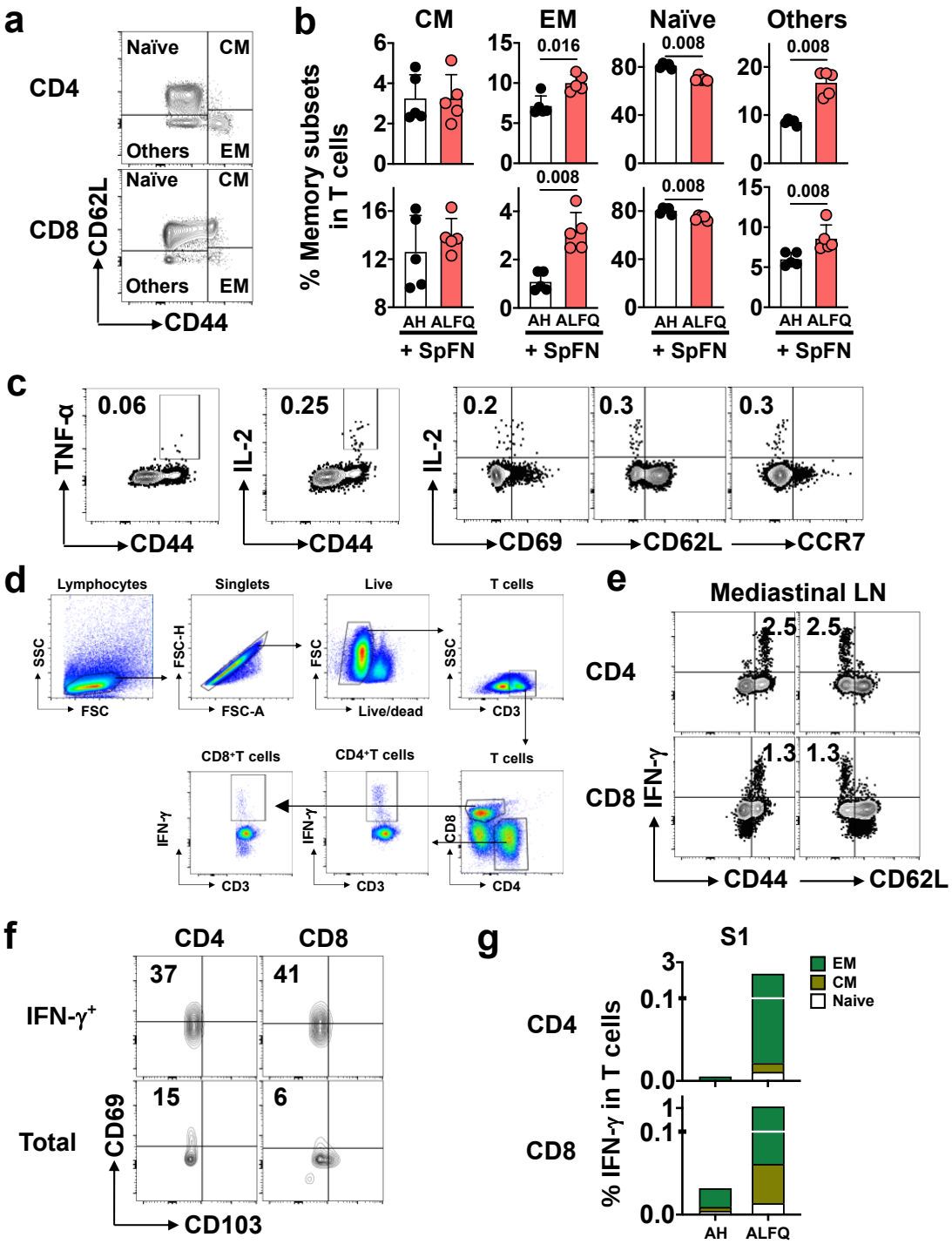

Supplementary Fig. 2. Characterization of responding T cells in lymph nodes after SpFN vaccination. (a) Early indication of memory potential phenotypes shown as flow plots (left panels) and quantitation of phenotype potential between the two vaccine groups at day 7 after the first vaccination (right panel) in the dLNs. **(b)** Memory potential was characterized as naive ($CD62L^+CD44^-$), central memory ($CD62L^+CD44^+$), effector memory ($CD62L^-CD44^+$), and other. **(c)** Cytokine expression and activation markers characterizing SARS-CoV-2 spike-specific $CD4^+$ T cells at day 10 day after the first vaccination. **(d)** Flow cytometry gating strategy for the identification of SARS-CoV-2 spike-specific $CD4^+$ and $CD8^+$ T cells in the mediastinal LNs at week 6 post prime-boost vaccination. **(e-f)**, Characterization of the SARS-CoV-2 spike-specific $CD4^+$ and $CD8^+$ T cells in the mediastinal LNs at week 6 following prime-boost vaccination by the expression of IFNγ. $IFN\gamma^+$T cells are **(e),** $CD44^+CD62L^-$ and **(f)** more frequently $CD69^+$ than parent populations, but $CD103^-$, indicating activated status. **(g)** Memory phenotype of $IFN\gamma^+$T cells in the mediastinal LN 6 weeks post-vaccination. Bars indicate mean ± s.d. Differences between the two groups were analyzed by using non-parametric Mann–Whitney U-test with $P \leq 0.05$ considered as statistically significant.

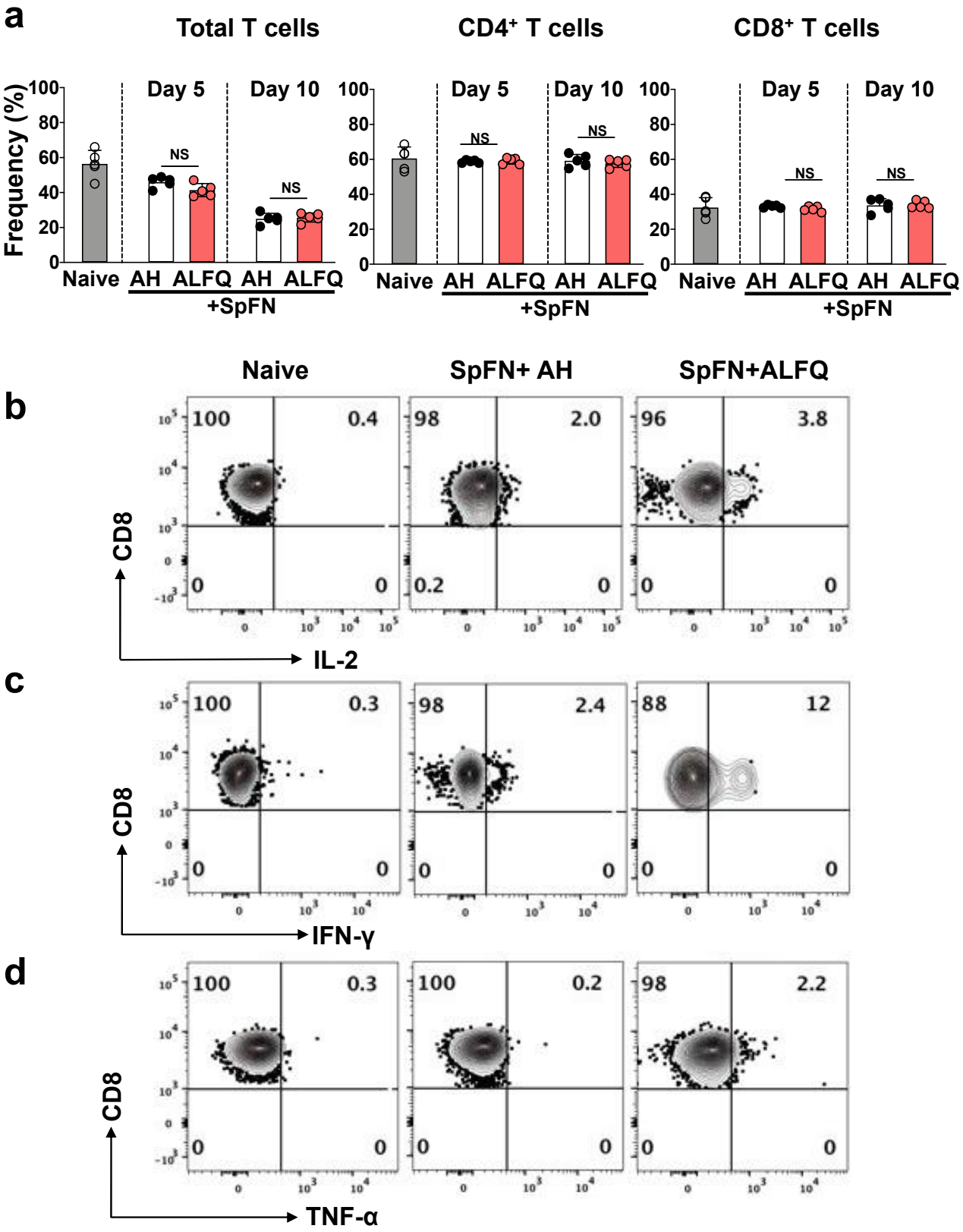

Supplementary Fig. 3. Frequency of T cells in splenocytes of mice following priming vaccination with SpFN vaccine. **(a)** Frequency of total $CD3^+$, $CD4^+$ and $CD8^+$ T cells in splenocytes of mice on days 5 and 10 post priming vaccination with SpFN adjuvanted with AH or ALFQ. **(b-d)** Representative flow plots depicting the frequency of **(b)** IL-2 **(c)** IFN-γ and **(d)** TNF-α secreting $CD8^+$ T cells on day 10 post priming vaccination. Bars indicate mean ± s.d.

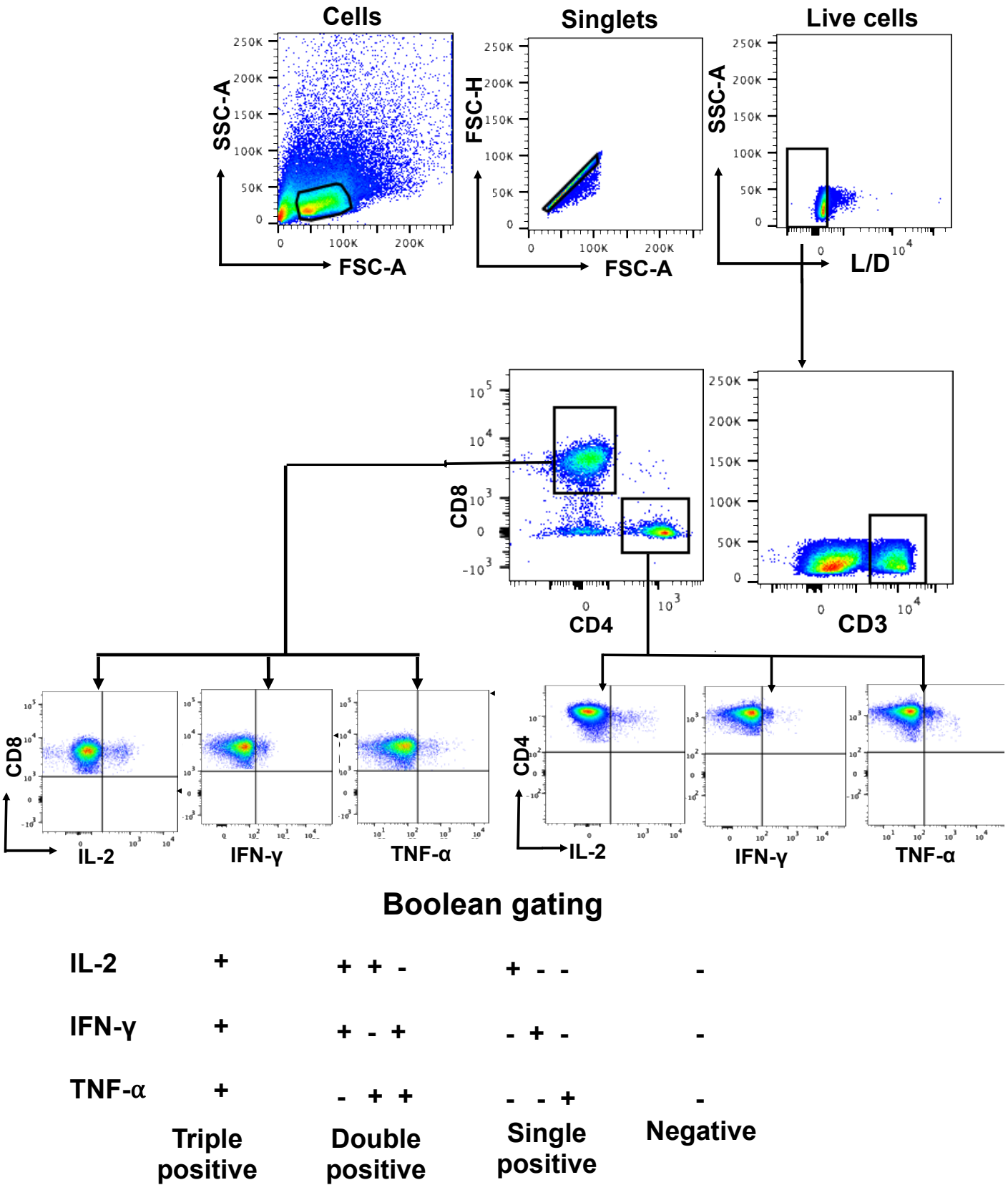

Supplementary Fig. 4. Flow gating strategy to determine the frequency of cytokine secreting CD4⁺ and CD8⁺ T cells. Flow gating strategy to determine the frequency of cytokine secreting IL-2, IFN-γ, and TNF-α secreting CD4⁺ and CD8⁺ T cells. Gates were defined on the respective fluorescence minus one (FMO) control. Boolean gating was performed to identify single, double, and triple positive intracellular cytokine positive cells.

1 59
MFVFLVLLPLVSSQCVNLTTRTQLPPAYTNSFTRGVYYPDKVFRSSVLHSTQDLFLPFF
60 119
SNVTWFHAIHVSGTNGTKRFDNPVLPFNDGVYFASTEKSNIIRGWIFGTTLDSKTQSLLI
120 179
VNNATNVVIKVCEFQFCNDPFLGVYYHKNNKSWMESEFRVYSSANNCTFEYVSQPFLMDL
180 239
EGKQGNFKNLREFVFKNIDGYFKIYSKHTPINLVRDLPQGFSALEPLVDLPIGINITRFQ
240 299
TLLALHRSYLTPGDSSSGWTAGAAAYYVGYLQPRTFLLKYNENGTITDAVDCALDPLSET
300 359
KCTLKSFTVEKGIYQTSNFRVQPTESIVRFPNITNLCPFGEVFNATRFASVYAWNRKRIS
360 419
NCVADYSVLYNSASFSTFKCYGVSPTKLNDLCFTNVYADSFVIRGDEVRQIAPGQTGKIA
420 479
DYNYKLPDDFTGCVIAWNSNNLDSKVGGNYNYLYRLFRKSNLKPFERDISTEIYQAGSTP
480 539
CNGVEGFNCYFPLQSYGFQPTNGVGYQPYRVVVLSFELLHAPATVCGPKKSTNLVKNKCV
540 599
NFNFNGLTGTGVLTESNKKFLPFQQFGRDIADTTDAVRDPQTLEILDITPCSFGGVSVIT
600 659
PGTNTSNQVAVLYQDVNCTEVPVAIHADQLTPTWRVYSTGSNVFQTRAGCLIGAEHVNNS
660 719
YECDIPGAGICASYQTQTNSPRRARSVASQSIIAYTMSLGAENSVAYSNNSIAIPTNFTIS
720 779
VTTEILPVSMTKTSVDCTMYICGDSTECSNLLLQYGSFCTQLNRALTGIAVEQDKNTQEVF
780 839
AQVKQIYKTPPIKDFGGFNFSQILPDPSKPSKRSFIEDLLFNKVTLADAGFIKQYGDCLGD
840 899
IAARDLICAQKFNGLTVLPPLLTDEMIAQYTSALLAGTITSGWTFGAGAALQIPFAMQMA
900 959
YRFNGIGVTQNVLYENQKLIANQFNSAIGKIQDSLSSTASALGKLQDVVNQNAQALNTLVK
960 1019
QLSSNFGAISSVLNDILSRLDKVEAEVQIDRLITGRLQSLQTYVTQQLIRAAEIRASANLA
1020 1079
ATKMSECVLGQSKRVDFCGKGYHLMSFPQSAPHGVVFLHVTYVPAQEKNFTTAPAICHDGK
1080 1139
AHFPREGVFVSNGTHWFVTQRNFYEPQIITTDNTFVSGNCDVVIGIVNNTVYDPLQPELDS
1140 1199
FKEELDKYFKNHTSPDVDLGDISGINASVVNIQKEIDRLNEVAKNLNESLIDLQELGKYEQ
1200 1259
YIKWPWYIWLGFIAGLIAIVMVTIMLCCMTSCCSCLKGCCSCGSCCKFDEDDSEPVLKGVKL
1260
HYT

Supplementary Fig. 5. Amino acid sequence of the SARS-CoV-2 spike protein.
Highlighted peptides were part of ELISpot-reactive SARS-CoV-2 glycoprotein derived matrix peptide pools. Underlined peptides are sequences predicted by NETMHC prediction algorithm (iedb.org). Numbers indicate amino acid residues.

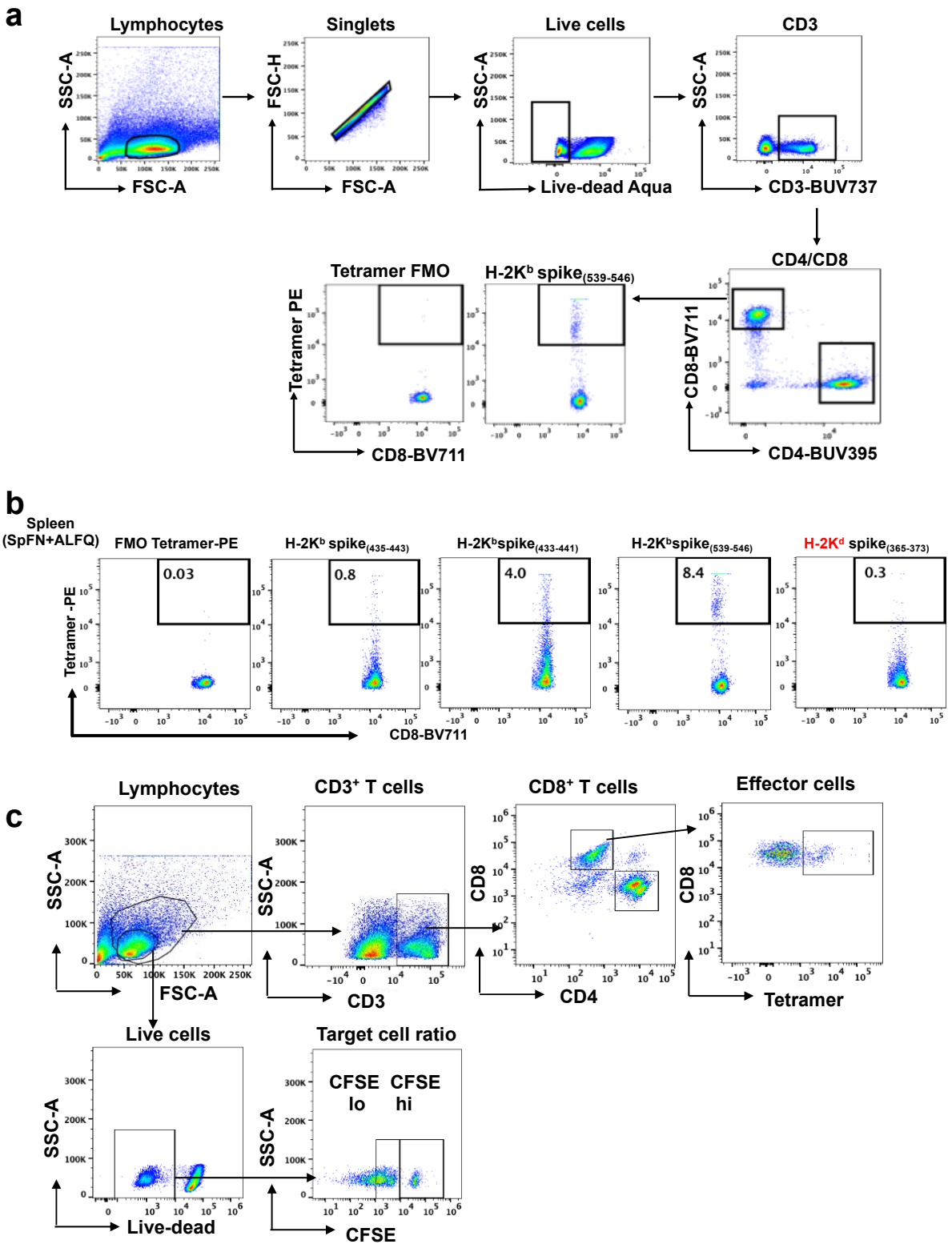

Supplementary Fig. 6. Flow gating strategy for determining the frequency of SARS-CoV-2 specific CD8$^+$ T cells and for the CTL assay following SpFN vaccination

(a) Flow gating strategy to determine the frequency of SARS-CoV-2 spike specific CD8$^+$ T cells in the splenocytes of SpFN vaccinated mice as detected by MHC class I tetramer staining**. (b)** Cells were stained for four different tetramers directed towards four different epitopes on SARS-CoV-2 spike protein [K^b $_{(433-441)}$; $_{(435-443)}$; $_{(539-546)}$ and K^d $_{(365-373)}$]. Detailed information is provided in Supplementary Table 6. **(c)** Gating strategy used to determine the frequency of tetramer positive CD8$^+$ T cells (effector cells) and ratio of CFSE high (hi): low (lo) target cells in the cytotoxic T lymphocyte killing assay.

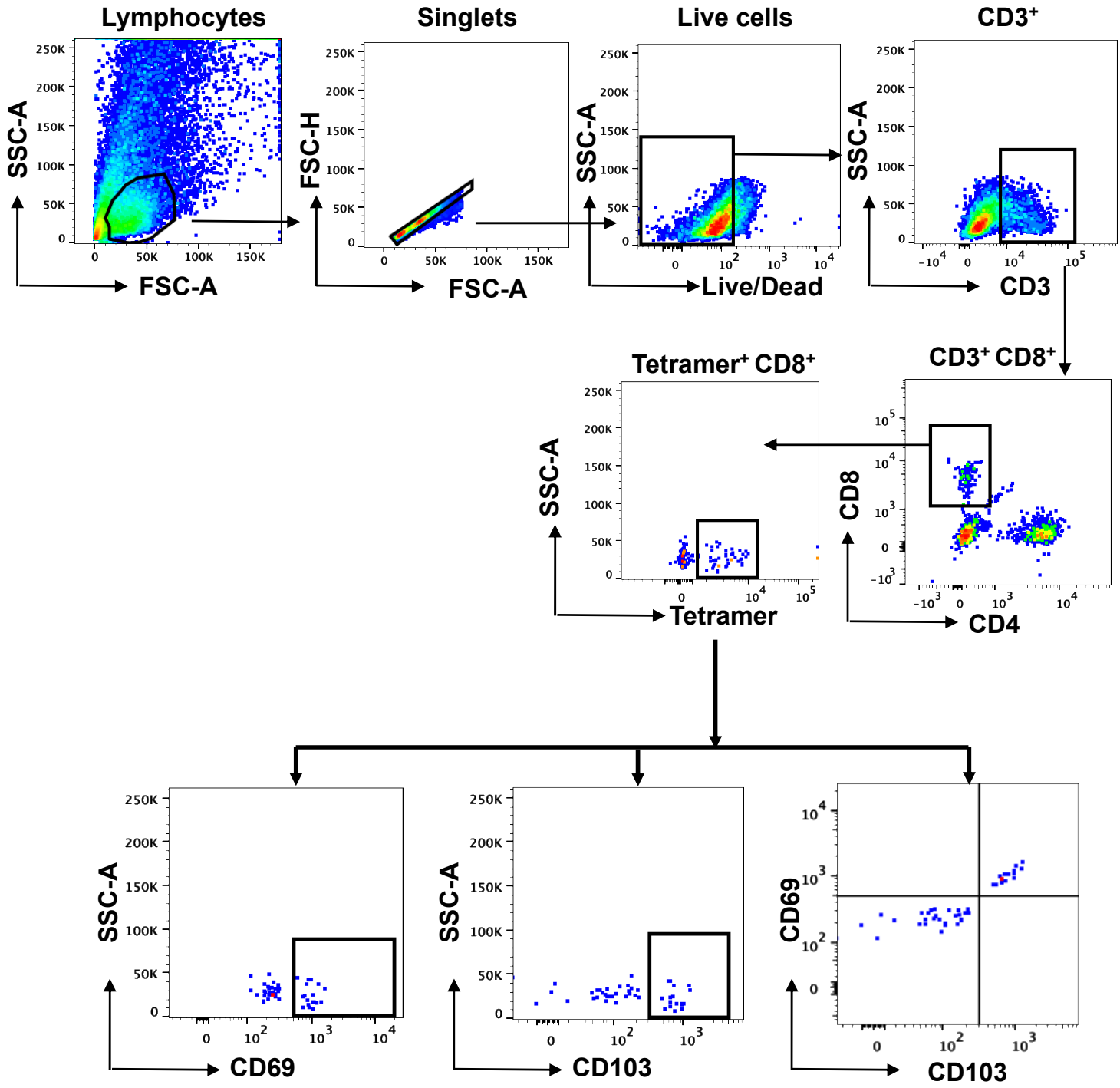

Supplementary Fig. 7. Flow gating strategy to determine the frequency of SARS-CoV-2 spike-specific CD8⁺ T cells in perfused lungs of SpFN vaccinated mice as detected by MHC class I tetramer staining followed by CD69 and CD103 staining. Flow gating strategy to determine the frequency of SARS-CoV-2 spike $_{(539\text{-}546)}$-specific tetramer positive CD8⁺ T cells followed by CD69 and CD103 staining in lung tissue of SpFN vaccinated mice.

Supplementary Table 1. List of antibodies used for Cytex flow cytometry-based analysis of the APC phenotypes

Antigen	Fluorochrome	Clone	Manufacturer	Catalog number
CD45R/B220	BUV395	RA3-6B2	BD	563793
CD80	BUV661	16-10A1	BD	741515
CD3	BUV737	145-2C11	BD	612771
CD86	BUV805	GL1	BD	741946
CCR7	BV421	4B12	BioLegend	120120
CD40	BV480	3/23	BD	746970
XCR1	BV510	ZET	BioLegend	148218
CD11c	BV570	N418	BioLegend	117331
CD169	BV605	3D6.112	BioLegend	142413
F4/80	BV650	BM8	BioLegend	123149
I A/E	BV711	M5/114.15.2	BioLegend	107643
CD117	BV750	2B8	BD	747412
CD44	BV785	IM7	BioLegend	103059
CXCR5	FITC	L138D7	BioLegend	145520
CD8a	PerCP	53-6.7	BioLegend	100732
CD24	PerCP-Cy5.5	M1/69	BioLegend	101824
PDCA1	PE	REA818	Miltenyi Biotec	130-112-220
CD103	PE-Dazzle594	2E7	BioLegend	121430
CD11b	PE-Cy5	M1/70	BioLegend	101210
Siglec-F	PE-Vio770	REA798	Miltenyi Biotec	130-112-176
CD64	AF647	X54-5/7.1	BioLegend	139322
Ly6G	AF700	1A8	BioLegend	127610
NK1.1	APC-Cy7	PK136	BioLegend	108724
CD45	APC-Fire810	30-F11	BioLegend	103174

Supplementary Table 2. List of antibodies used for Cytex flow cytometry-based analysis of the T cell phenotypes

Antigen	Fluorochrome	Clone	Manufacturer	Catalog number
CD3	BUV395	145-2C11	BD	563565
CD69	BV421	H1.2F3	BioLegend	104528
CD44	BV510	IM7	BioLegend	103044
CD62L	BV570	MEL-14	BioLegend	104433
PD-1	BV605	29F.1A2	BioLegend	135219
ICOS	BV650	398.4A	BioLegend	313550
CD8	PerCP-Cy5.5	53-6.7	BioLegend	100734
CXCR5	PE	L138D7	BioLegend	145504
CD4	PE-Dazzle 594	GK1.5	BioLegend	100456
CCR7	PE-Cy5	4B12	BioLegend	120114
CD45	APC-Fire810	30-F11	BioLegend	103174

Supplementary Table 3. List of antibodies used for Cytex flow cytometry-based analysis of the T cell cytokine staining

Antigen	Fluorochrome	Clone	Manufacturer	Catalog number
T cell surface staining				
CD3	BUV395	145-2C11	BD	563565
CD69	BV421	H1.2F3	BioLegend	104528
CD44	BV510	IM7	BioLegend	103044
CD62L	BV570	MEL-14	BioLegend	104433
ICOS	BV650	398.4A	BioLegend	313550
CXCR3	BV711	CXCR3-173	BD	740825
CD8	PerCP-Cy5.5	53-6.7	BioLegend	100734
CXCR5	PE	L138D7	BioLegend	145504
CD4	PE-Dazzle 594	GK1.5	BioLegend	100456
CCR7	PE-Cy5	4B12	BioLegend	120114
PD-1	APC	29F.1A2	BioLegend	135210
CD45	APC-Fire810	30-F11	BioLegend	103174
T cell intracellular cytokine staining				
IFN-γ	BV605	XMG1.2	BioLegend	505839
TNF-α	BV785	MP6-XT22	BioLegend	506341
IL-2	FITC	JES6-5H4	BioLegend	503806
GrB	PE-Cy7	QA16A02	BioLegend	372214
IL-17A	AF700	TC11-18H10.1	BioLegend	506914
IL-10	APC-Cy7	JES5-16E3	BioLegend	505036

Supplementary Table 4. List of antibodies used for intracellular cytokine staining by BD LSRII flow cytometry-based analysis of the cytokine response in the splenocytes

Antigen	Fluorochrome	Clone	Manufacturer	Catalog number
CD3	BUV737	145-2C11	BD	612771
CD4	BUV395	GK1.5	BD	565974
CD8a	BV711	53-6.7	BD	563046
IFN-γ	V450	XMG1.2	BD	560661
IL-4	PerCP-Cy5	11B11	BD	560700
TNF-α	FITC	MP6-XT22	BD	554418
IL-2	APC	JES6-5H4	Biolegend	503810
IL-2	PE	JES6-5H4	Biolegend	503808

Supplementary Table 5. List of antibodies used for staining perfused lung cells and analysis by BD LSRII flow cytometry

Antigen	Fluorochrome	Clone	Manufacturer	Catalog number
CD3	BUV737	145-2C11	BD	612771
CD4	BUV395	GK1.5	BD	565974
CD8a	BV711	53-6.7	BD	563046
CD69	BV650	H1.2F3	BD	740460
CD103	BV510	2E7	BD	748258

Supplementary Table 6. List of MHC class I tetramer used for the detection of SARS-CoV-2 spike specific $CD8^+$ T cell response

Allele	Description[1]	Peptide sequence	Fluorochrome	Concentration
$H\text{-}2K^d$	SARS-CoV-2-spike aa 365-373	CYGVSPTKL	PE-labeled tetramer	1.1 mg/mL
$H\text{-}2K^b$	SARS-CoV-2-spike aa 433-441	GNYNYLYRL	PE-labeled tetramer	1.3 mg/mL
$H\text{-}2K^b$	SARS-CoV-2-spike aa 539-546	VNFNFNGL	PE-labeled tetramer	1.2 mg/mL
$H\text{-}2K^b$	SARS-CoV-2-spike aa 435-443	YNYLYRLF	PE-labeled tetramer	1.3 mg/mL

[1]The tetramers were obtained from NIH Tetramer Core Facility at Emory University, Atlanta, GA.